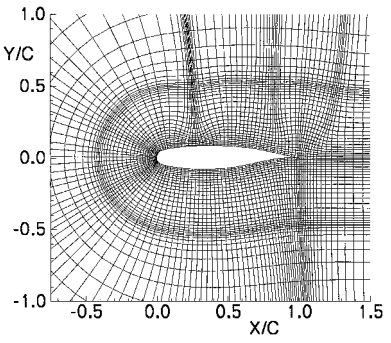

Fig. 3 Sample grid around NLR-7301 airfoil.

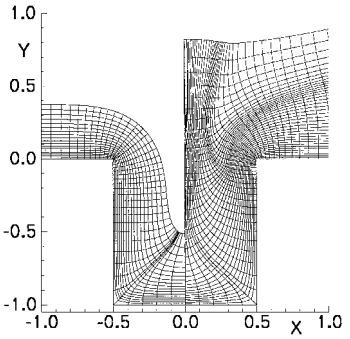

Fig. 4 Comparison of two grids generated around a cavity without ($X < 0.0$) and with ($X > 0.0$) using the present marching distance functions.

Results

To present the new method developed here, a sample grid was generated around the National Aerospace Laboratory- (NLR-) 7301 airfoil as shown in Fig. 3. For this grid, the surface clustering was applied by using $s_1/C = 0.01$ and $\varepsilon = 0.1$. The applications of the grid control for the interior domain are also presented. In Fig. 3, the additionally clustered lines in the η direction, the clustered lines in the ξ direction above the front-half of the airfoil, and the rarefied lines in the ξ direction above the trailing edge can all be easily observed.

In Fig. 4, two grids developed around a cavity are compared. The grid at the left side of the symmetry line ($X = 0.0$) was obtained without using the marching distance functions. For this grid, grid lines crossed after the 19th η level. The grid at the right side of the symmetry line was produced by using multiple controls in the ξ direction. The grid line crossings were eliminated, and a controlled interior point distribution was obtained. For both grids, all of the other parameters were exactly the same. For these cavity cases, some local imperfections were removed by applying a simple algebraic smoothing procedure after completion of the hyperbolic grids.

Conclusions

The marching distance functions, as presented here, can be used when there is a need for interior domain grid control, such as in problems with shocks or in problems with cavities where the generation of grids is relatively more difficult. They can also be useful for the solution adaptive grid generation procedures.

References

[1]Chan, W. M., "Hyperbolic Methods for Surface and Field Grid Generation," *Handbook of Grid Generation*, edited by J. F. Thompson, B. K. Soni, and N. P. Weatherill, CRC Press, Boca Raton, FL, 1999, pp. 5.1–5.26.

[2]Chan, W. M., and Steger, J. L., "Enhancements of a Three-Dimensional Hyperbolic Grid Generation Scheme," *Applied Mathematics and Computation*, Vol. 51, No. 1, 1992, pp. 181–205.

[3]Tai, C. H., Chiang, D. C., and Su, Y. P., "Three Dimensional Hyperbolic Grid Generation with Inherent Dissipation and Laplacian Smoothing," *AIAA Journal*, Vol. 34, No. 9, 1996, pp. 1801–1806.

P. Givi
Associate Editor

Ignition Mechanisms of Jet-A Fuel Vapor in a Confined Environment

Tae-Woo Lee*
Arizona State University, Tempe, Arizona 85287-6106

Introduction

IGNITION mechanisms of jet-A fuel vapor are of interest for safety reasons during storage in aircraft fuel tanks. Fuel vapor is present in the ullage (air space above the remaining fuel) of all fuel tanks. Fuel vapor can accumulate in fuel tanks as fuel consumption increases the empty volume in the tank. Under certain flight and ground conditions, the fuel vapor mixed with the available air in the tank is within flammable limits. Some recent work has been done by Shepherd et al.,[1] but current data on ignition characteristics of jet fuels are far from complete. In addition, the ignition mechanisms in confined environments with realistic probability of occurrence need to be identified correctly and eliminated.

The necessity to obtain data on ignition mechanisms and so-called minimum ignition energy of jet-A fuel vapor has recently been reemphasized due to the highly publicized incident involving TWA flight 800. Whereas the frequency of such an incident is very small, these events are unpredictable and catastrophic in nature. Also, any measure that is taken to minimize an ignition event in aircraft fuel tanks should be based on quantitative data on jet-A fuel vapor flammability, as well as on an understanding of the origin of these ignition events.

Ignition is a much explored area in combustion science, and numerous studies have been devoted to characterizing ignition of gas- and liquid-phase fuels (see Refs. 2–7 as examples). However, studies of jet-A fuel vapor for applications in fuel tank safety have been relatively few, uncorrelated with one another, and at times with insufficiently defined test conditions. Only in the recent past have more careful reports summarizing jet-A fuel vapor flammability been published.[1,8] Both the reports by Hill[8] and Shepherd et al.[1] include a review of the previous historical measurements[9–11] of jet-A fuel vapor flammability limits. Some of the factors that make the use of the previous data on jet-A fuel vapor flammability difficult are 1) undefined fuel batch flashpoint or other fuel characteristics, 2) variations in the criterion for fuel vapor ignition, 3) variations in the electrode configurations and spark deposition modes (spark duration, etc.), 4) differences in the test chamber scale/geometry and, therefore, fuel thermal conditions, and 5) undefined fuel loading or variations thereof.

Recent data reported by Shepherd et al.[1] and Naegeli and Childress[12] offer more information on the jet-A fuel vapor ignition limits under well-defined conditions. However, because the focus of the report by Shepherd et al.[1] was on determination of the cause of the TWA 800 accident, it did not necessarily include a coverage of conditions generally applicable for all of the phases of a flight. The work by Naegeli and Childress[12] mostly involves a comparison of different jet fuels and correlation with their chemical contents.

Here, we report on ignition limits of jet-A fuel vapor as a function of the fuel loading using conventional electrical sparks. In addition, we present a much more relevant ignition mechanism for accidental ignition events involving electrical contact sparks and demonstrate its capability to ignite fuel–air mixtures at very low voltage and power settings.

Experimental Methods

Combustion Chamber

The combustion chamber consisted of a three-port, stainless-steel chamber for atmospheric to vacuum operations. The chamber had

Received 15 February 2000; revision received 11 June 2000; accepted for publication 12 June 2000.

*Associate Professor, Department of Mechanical and Aerospace Engineering.

a diameter of 100 mm, length of 270 mm, and flange diameter of 150 mm, whereas the smaller port had a diameter of 75 mm, length of 73 mm, and flange diameter of 120 mm. The chamber had a pressure rating of ultra-high vacuum (10^{13} torr), and the total internal volume was 2.2 liter. The chamber pressure and temperature could be independently controlled. Further details of the experimental setup will be published elsewhere.

The electrodes were machined from stainless steel. They were 3 mm ($\frac{1}{8}$ in.) in diameter × 230 mm in length, with one end threaded for electrical connection. The electrodes had a 15-deg taper and were pointed at the end. The electrodes were mounted and electrically insulated from the chamber using CONAX compression fitting (model EGT-125-A) and accompanying Teflon® liners. The spark gap was fixed at 4 mm for the conventional electrical sparks, and for electrical contact sparks, one of the electrodes was kept stationary while the other moved toward and back from the contact point.

Ignition Systems

Two different ignition mechanisms were investigated. One was a conventional electrical spark ignition system involving inductance-coil (Wells C835) and a solid-state switching relay (Wells DR100). The electrical sparks were measured to have a spark duration of approximately 3 ms and a nominal spark energy of 39 mJ for a typical spark. The spark characteristics were measured with a high-voltage probe and a current sensor, connected to a high-speed oscillopscope that recorded the traces for later integration. The measured spark characteristics were quite similar to typical sparks generated by automotive inductance-coil systems, with a breakdown voltage peaking at 3–4 kV range and then continuing at lower voltages during the glow discharge phase. A second ignition mechanism, potentially much more relevant for accidental ignition, is a system in which one of the electrodes was allowed to traverse and come in contact with a stationary electrode, producing sparks at very low supply voltages (as low as 2 V). As the electrodes moved away, the heat generated from the sparks was efficiently transferred to the surrounding causing an ignition.

Test Conditions and Data Accuracy

Three parameters were considered, pressure (altitude), temperature, and fuel loading. The pressure ranged from 1 atm (0-ft altitude) to 0.2 atm (38 kft), while the temperature varied from approximately 25°F below to 40°F above the flashpoint (temperature at which a standard mixture is observed to ignite in specified test arrangement. The current jet-A fuel batch had a measured flashpoint of 122°F, using American Society for Testing and Materials D56 Pensky–Marten closed-cup method. The fuel loading changed from 0.7 (2 ml in 2.2-liter chamber) to 147 kg/m^3 (400 ml in 2.2-liter chamber). The pressure variation is of course to determine the effects of altitude, whereas a range of fuel loading is considered because the fuel quantity can vary in aircraft fuel tanks. Note that due to the industry custom Farenheit temperature units have been used throughout this paper in place of the standard SI units.

The ignition temperature measurements involved incrementing the chamber temperature in 2.5°F increments and applying sparks until ignition was observed. Thus, the accuracy is expected to be within 2.5°F, but the temperature data were otherwise quite repeatable. The chamber temperature was uniform in the central region within 2–3°F; however, due to unavoidable heat loss at the wall, the temperature tended to be lower near the wall by 5–10% of the target temperature. Because the ignition sparks were applied at the center of the chamber, well away from the wall regions, this is not expected to affect the accuracy of the data in any significant manner.

Results and Discussion

The pressure during ignition event was monitored, and traces showed a sharp spike with the pressure increasing by approximately a factor of six from the initial pressure. This corresponds to a temperature increase of a factor of six, consistent with the typical temperature increase during hydrocarbon combustion under constant-volume conditions. The ignition temperature was measured and recorded when there is such a full pressure increase due to ignition of the fuel vapor. Evidence of partial pressure increase was checked for the range from −2.5 to −5°F of the observed ignition temperature; however, no such partial ignition phenomenon was observed.

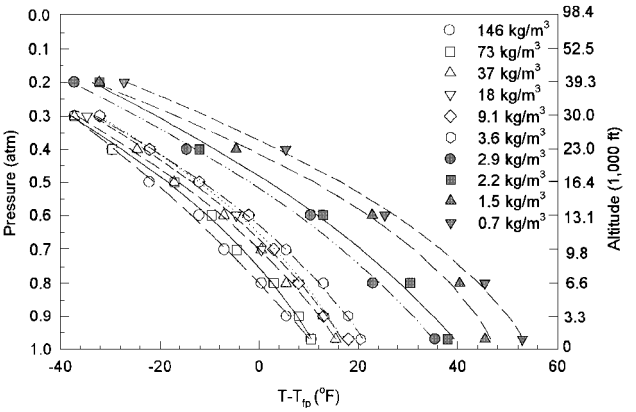

Fig. 1 Ignition limits of jet-A fuel vapor at various fuel loadings; inductance-coil ignition circuitry is used with the fuel flashpoint T_{fp} of 122°F.

Conventional Electrical Spark Ignition

The ignition limits of jet-A fuel vapor, using conventional electrical sparks, are shown in Fig. 1 for a range of fuel loading from 0.7 to 146 kg/m^3. Here, the fuel loading refers to the mass of fuel divided by the total chamber volume. Again, note that due to industry custom, Fahrenheit temperature units have been used in place of standard SI units. The data included in Fig. 1 are the lower ignition limits corresponding to the lean flammability limits. The ignition temperatures have been shifted by the reference fuel flashpoint. The ignition temperature decreases with decreasing pressure (increasing altitude) because the chamber is filled initially filled with liquid fuel that is allowed to come to an equilibrium at given pressure and temperature. At lower pressures, more fuel vapor relative to the air mass is present at a given temperature to shift the equivalence ratio closer to stoichiometry. Therefore, the traces of ignition limits has a negative slope in Fig. 1, typical of liquid–vapor mixture ignition behavior. Observe that there is a substantial effect of the fuel loading on the ignition temperature. As the fuel loading decreases, the ignition temperature increases.

Alternative Ignition Mechanism in Fuel Tanks

One question that arises is, how are the sparks produced in a confined environment such as fuel tanks that can cause ignition under these conditions? Conventional studies of ignition have typically involved sparks from electrical breakdown at high voltages (3 kV and above) or laser sparks. For the cause of accidental ignition in environments such as aircraft fuel tanks where the electrical power supplied to devices such as fuel quantity indicators and fuel pumps is limited for safety reasons, the probability of multiple malfunctions that can lead to an electrical potential of 3 kV is nearly nonexistent. We present another possible ignition mechanism that can occur at much lower voltages and, therefore, present a much more probable ignition threat. If two charged electrodes come in contact with another and move away after the contact, rather intense sparks can be generated at very low voltage and current. The motion of the electrode away from the spark allows sufficient heat transfer to the surrounding for an ignition. We refer to this phenomenon as electrical contact spark. During the near-contact phase of the collision of anode and cathode, the proximity of the electrodes can allow the electrons to jump across causing a plasmalike condition for a short duration due to the streaming of electrons. Also, the collision impact at the electrode surface itself can generate free electrons that stream toward the anode. If the electrodes move away from one another, the thermal energy released during this spark is not absorbed by the electrodes and it gets transported to the surrounding gas phase causing an ignition. This is a dynamic ignition mechanism, in contrast to the conventional sparks generated by stationary electrodes, that has not received any research attention in the context of fuel

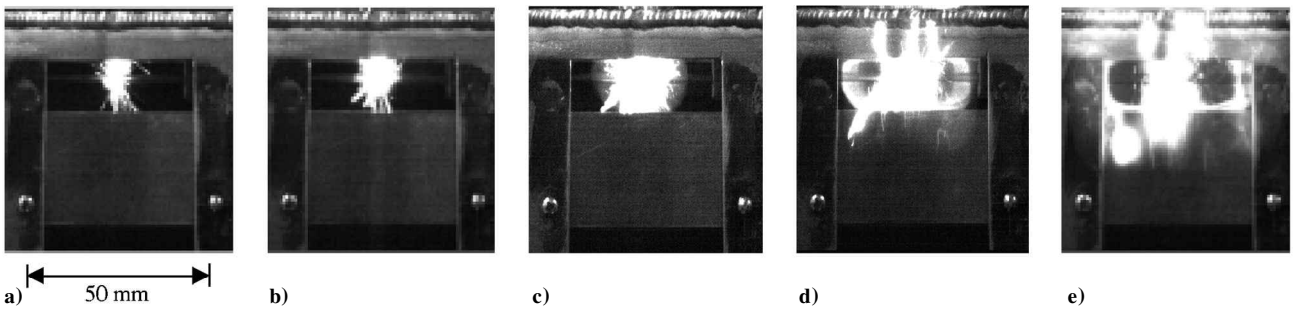

Fig. 2 Sequence of electrical contact sparks causing an ignition of methane–air mixture.

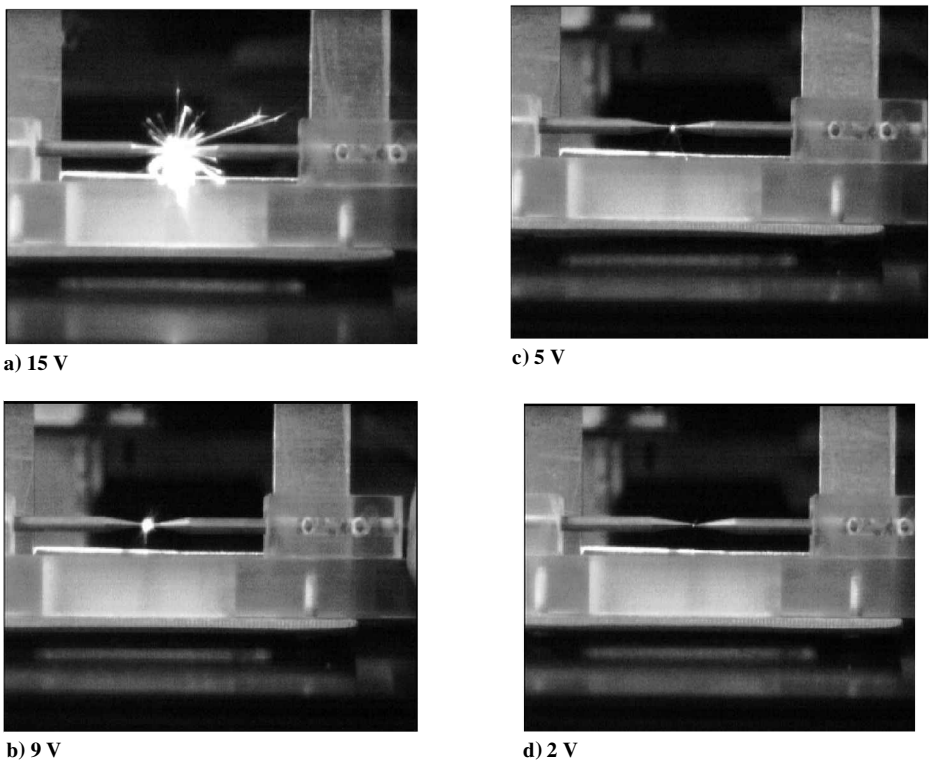

Fig. 3 Electrical contact sparks at various voltage settings.

vapor ignition. Indeed, Fig. 2 demonstrates the ignitability of fuel–air mixture due to this spark mechanism in methane–air mixture at equivalence ratio of 1. The mixture was at low mean velocity (less than 0.4 m/s) and, thus, is not expected to be a factor. Figures 2a–2e show the development of the flame kernel arising from the spark in Fig. 2a. The time interval is approximately 100 ms from one image to the next. From Fig. 2c the flame kernel can be observed with subsequent propagation toward the chamber wall in Fig. 2e.

The electrodes that were used in these experiments were similar to the one used to obtain the ignition limits in Fig. 1, with a 3-mm diam sharpened with a 15-deg taper at the ends. The geometry of the electrodes will have a significant influence because the heat conduction increases with increasing electrode diameter. In fact, tests with a flat electrode colliding with a sharpened one yielded no ignition events, due to increased heat loss at the flat end. If the electrodes are smaller in diameter, it is likely that ignition can occur at yet lower supplied electrical energy. A possible event, thus, is a bare electrical wire, intermittently shorting to create sparks of this type, even at very low electrical energy levels and causing an ignition of the fuel vapor. The sparks themselves could be observed at voltages as low as 2 V. Figure 3 shows these sparks at various voltage settings starting from 15 V in Fig. 3a to 2 V in Fig. 3d. The current setting was nominally 1 A for closed circuit.

Conclusions

Ignition behavior of jet-A fuel vapor has been determined for the effects of fuel loading and fuel flashpoint. Two different ignition mechanisms were investigated. One is a conventional electrical spark circuitry (39-mJ spark energy, 3-kV breakdown voltage). Using this spark source, the temperature at which ignition occurred varies from −10 to +55°F of the flashpoint, depending on the fuel loading, and decreases with decreasing pressure for all fuel loadings. A second ignition mechanism that has been demonstrated involves sparks that are produced when electrodes collide with one another, even at very low supplied voltages (as low as 2 V). Because the conventional electrical sparks require a breakdown voltage of 3 kV and above, the latter type of sparks is considered to be a much more probable cause of accidental ignition of fuel vapor. Indeed, tests in a methane–air mixture shows that ignition occurs with supplied voltages of as low as 15 V, with possibilities existing at even lower spark energies, depending on the electrode geometry and electrode collision dynamics.

Acknowledgments

Contributions to the experimental set up and test data were made by Vivek Jain, Stuart Kozola, Manjunath Hanumanthappa, Tenghai Wang, and Sangjun Lee.

References

[1] Shepherd, J. E., Krok, J. C., and Lee, J. J., "Jet A Explosion Experiments: Laboratory Testing," Explosion Dynamics Lab. Rept. FM97-5, prepared for National Transportation Safety Board, California Inst. of Technology, Pasadena, CA, 1997.

[2]Ballal, D. R., and Lefebvre, A. H., "Ignition and Flame Quenching of Flowing Heterogenous Fuel-Air Mixtures," *Combustion and Flame*, Vol. 35, 1979, p. 155.

[3]Ballal, D. R., and Lefebvre, A. H., "Ignition of Liquid Fuel Sprays at Subatmospheric Pressures," *Combustion and Flame*, Vol. 31, 1978, p. 115.

[4]Ballal, D. R., and Lefebvre, A. H., "Spark Ignition of Turbulent Flowing Gases," AIAA Paper 77-185, 1977.

[5]Kono, M., Kumagai, S., and Sakai, T., "Optimum Condition of Ignition of Gases by Composite Sparks," *Sixteenth Symposium (International) on Combustion*, Combustion Inst., Pittsburgh, PA, 1978, p. 757.

[6]Ziegler, G. F. W., Wagner, E. P., and Maly, R. P., "Ignition of Lean Methane–Air Mixtures by High Pressure Glow and Arc Discharges," *Twentieth Symposium (International) on Combustion*, Combustion Inst., Pittsburgh, PA, 1984, p. 1817.

[7]Maly, R. P., "Spark Ignition," *Fuel Economy*, edited by J. C. Hilliard and G. S. Springer, Plenum, New York, 1984, pp. 121–191.

[8]Hill, R., "A Review of the Flammability Hazard of Jet A Fuel Vapor in Civil Transport Aircraft Fuel Tanks," Federal Aviation Administration, Final Rept. DOT/FAA/AR-98/26, 1998.

[9]Kuchta, J. M., "Summary of Ignition Properties of Jet Fuels and Other Aircraft Combustible Fluids," TR AFAPL-TR-75-70, U.S. Bureau of Mines, 1975.

[10]Nestor, L., "Investigation of Turbine Fuel Flammability Within Aircraft Fuel Tanks," Naval Air Propulsion Test Center, Final Rept. DS-67-7, Naval Base, Philadelphia, 1967.

[11]Ott, E., "Effects of Fuel Slosh and Vibration on the Flammability Hazards of Hydrocarbon Turbine Fuels Within Aircraft Fuel Tanks," Air Force Aero Propulsion Lab., TR AFAPL-TR-70-65, Wright–Patterson AFB, OH, 1970.

[12]Naegeli, D. W., and Childress, K. H., "Lower Explosion Limits and Compositions of Jet Fuel Vapors," Spring Technical Meeting of the Western States Sec., Combustion Inst., 98S-66, 1998.

J. P. Gore
Associate Editor

Ply Angle Optimization of Nonuniform Composite Beams Subject to Aeroelastic Constraints

Thomas Evrard,* Richard Butler,† and Steven W. Hughes‡
University of Bath, Bath, England BA2 7AY, United Kingdom
and
J. Ranjan Banerjee§
City University, London, England EC1V OHB, United Kingdom

I. Introduction

SEVERAL studies on the optimization of aeroelastically constrained, composite wings with cantilever end conditions have been conducted. For example, recent optimizations[1,2] have examined the design of nonuniform, flat composite beams for frequency, flutter, and divergence constraints. During these studies, variation of the thickness of a generic layup with fixed values of ply angles was considered, and an experimental validation was carried out. Other related work[3–6] has investigated the influence that ply orientation, sweep angle, wash-in, and wash-out, as well as various other parameters, has on flutter speed. This work showed that modal interchange can significantly alter the flutter speed of a composite wing[4] and that for flutter of an unswept composite wing, torsional rigidity and coupled bending–torsional rigidity[5] are the most influential parameters. It was also found that, contrary to traditional thinking, wash-out can be beneficial from a flutter point of view.[6] A recent independent study[7] has examined the effect of both ply angle variation and the position of lumped masses on flutter speed for uniform thickness wind-tunnel models. Here, the principal findings were that small variations in thickness can have a significant effect on flutter speed and that practical application of optimization should allow for uncertainties in the aerodynamic and structural models.

For all of the cited studies in which ply angle has been varied, the layup has been constructed from either unidirectional material [0 deg] or woven $[0/90]_S$ material. Also, the wing structure has previously consisted of a flat composite beam of uniform thickness. The current paper presents results in two parts, both of which are based on the model that has previously been optimized[1,2] and, in one case, experimentally tested.[1] The first part examines the effect that varying the orientation α of a $[90+\alpha/0+\alpha/+45+\alpha/-45+\alpha]_S$ layup has on the flutter and divergence speeds of a uniform beam that is both unswept and swept back, where the effect of such variation is to alter the influence of each layer on the beam rigidities. In the second part, the design optimization of nonuniform beams with varying orientation of the same layup is considered. The wing model consists of 10 uniform beam elements, where each element has a layup of $[90+\alpha/0+\alpha/+45+\alpha/-45+\alpha]_S$, a length of 0.04 m, and a width of 0.08 m (Fig. 1). The layup orientation α, which was previously[1,2] always 0 deg, is defined as the angle that the 0-deg fibers are inclined to the y axis of the beam. (Note that for a swept wing the y axis is the centroidal axis of the beam.) The structural beam is enclosed in a NACA 0015 airfoil of (unswept) chord 0.195 m. The mid-chord position of this airfoil is positioned 0.04 m in front of the beam center.

Analysis and optimization are described in detail in Ref. 2. Briefly, the dynamic stiffness method (DSM) is used to carry out free vibration analysis for the nonuniform composite beam by idealizing it as a series of uniform beam elements with bending, torsional, and coupled bending–torsional rigidities, EI, GJ, and K, respectively, where positive K causes the wing to twist leading edge down when it is bent upward. The effect of shear deformation, which is ignored in the model, is relatively small because DSM frequencies are relatively close to experimental and finite element results that allow for shear deformation.[1] The flutter speed V_f is found using the V–g method and the divergence speed V_d is obtained by considering it as a static (zero-frequency) instability problem.

II. Results

A. Parametric Study for Uniform Thickness Beam

The analysis of a uniform thickness beam model for varying layup orientation α, where each of the eight layers within the $[90+\alpha/0+\alpha/+45+\alpha/-45+\alpha]_S$ layup has the same thickness, is first considered. Figure 2 shows the variation of flutter and divergence speed with varying α for an unswept wing. (Here, as in Fig. 3, airspeed has been normalized against the flutter speed found when $\alpha = 0$ deg.) The maximum flutter speed occurs at around $\alpha = 52$ deg,

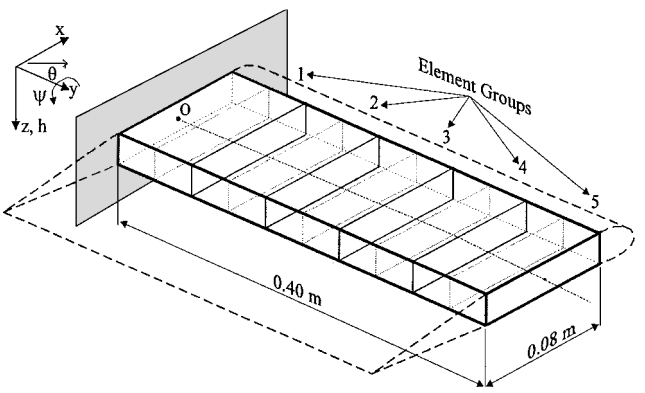

Fig. 1 Unswept wing model with coordinate system, where θ shows the direction of both positive layup orientation and positive ply angle.

Received 31 July 1999; revision received 16 April 2000; accepted for publication 6 June 2000.

*Placement Student, Department of Mechanical Engineering; currently Student, French Institute for Advanced Mechanical Engineering, Campus des Cezeaux, B.P. 265, 63175 Aubiere Cedex, France.

†Senior Lecturer, Department of Mechanical Engineering.

‡Student, Department of Mechanical Engineering.

§Reader, Department of Mechanical Engineering and Aeronautics.